ENGINEERING RESEARCH INSTITUTE
THE UNIVERSITY OF MICHIGAN
ANN ARBOR

Interim Report No. 1

# PRELIMINARY RESULTS ON THE TURBULENT MIXING OF SUPERSONIC JETS

A. M. Kuethe
H. E. Bailey

Aeronautical Engineering Department

Project 2270

DEPARTMENT OF THE AIR FORCE
WRIGHT AIR DEVELOPMENT CENTER
WRIGHT-PATTERSON AIR FORCE BASE, OHIO
CONTRACT AF 33(616)-2403, PROJECT NO. 54-610-185

September 1955

TABLE OF CONTENTS

## ABSTRACT

The report contains a description of the design procedure and of the apparatus as constructed, an exposition of the pertinent theory under the simplifications of linear analysis and preliminary results for one configuration.

## OBJECTIVE

The aim of the present work on supersonic jet mixing is to determine the effects of various factors such as stagnation temperature and pressure, Mach number, Reynolds number, and boundary-layer thickness on the mixing process and origin of disturbances forward of the jet lip.

## INTRODUCTION

The current study of supersonic jet mixing, on which this is an interim report, has for its objective the determination of the effects of various factors, such as stagnation temperature and pressure, Mach number, Reynolds number, and boundary-layer thickness, on the details of the mixing process and on the propagation of disturbances forward of the jet lip. We are restricting ourselves for the present to the two-dimensional mixing of two supersonic streams over a wide range of the above variables; however, the experimental apparatus can readily be adapted to the study of supersonic-subsonic and even subsonic-subsonic mixing.

This report is a description of the design procedure and of the apparatus as constructed, an exposition of the pertinent theory under the simplifications of linear analysis, and preliminary results for one configuration. The voluminous literature on jet mixing is referred to only insofar as it applies directly to the specific problems being investigated. Extensive bibliographies on mixing phenomena are available,[1,2] so it did not seem necessary to relist the many references.

## DESIGN CONSIDERATIONS AND DESCRIPTION OF APPARATUS

The mixing phenomena are studied in the region downstream of the lip at which two supersonic streams merge. The supersonic streams are generated by means of a double-corner nozzle as shown in Fig. 1. Figure 2 is a photograph of the setup with one side of the settling chamber removed, showing a side view of the honeycomb. Figure 3 shows the two channels with one of the tunnel side plates removed.

The double channel is 4 in. wide and the vertical dimensions of the upper and lower streams are respectively 4 in. and 2 in. The nozzle blocks are made of normalized SAE 1045 steel which gives a yield strength of approximately 50,000 psi. The coordinates of the contoured nozzle blocks are those obtained from Reference 3 and permit a variation of Mach number in each channel of from 1.4 to 4.0 by translation of the lower block with respect to the upper block.

In order to insure sufficient strength in the tip of the cantilevered middle nozzle block, it was necessary to rotate the lower contour of the mid-

dle nozzle block 1°. This causes the secondary jet to impinge on the main jet at an angle of 1°. This inclination is in addition to that prescribed by the rate of boundary-layer growth, which amounts to about 1.5°. The total inclination is therefore 2.5°. Since both streams are supersonic, the small degree of nonparellelism of the main streams will be adjusted by the shocks and expansions at the lip.

The construction involved modification of the corner nozzle developed under contract No. AF 33(038)-23070. The lower contour and the center block were adapted to the existing upper contour.

The maximum stress in the middle nozzle block, assuming a uniform air load of 5 psi, occurs 1-3/4 in. upstream of the lip and has a value of 3400 psi. The deflection of the lip, which is .025 in. thick, is .026 in. under this load. It should be mentioned here that the load of 5 psi is considerably larger than the actual load since, when the two nozzles are in operation, the static pressures on the upper and lower surfaces of the middle nozzle block are nearly equal, even though their ratio may be high.

The contours of both nozzle blocks were checked with a vernier height gauge by measuring from a fixed, ground, flat surface. In addition, the curvature of all the contoured surfaces was checked with the curvature gauge of Reference 3.

The nozzle blocks were aligned by setting the angles of the straight portions in the throat and in the test section at the values indicated in Reference 3, and at the same time setting the test-section height to the proper value. This alignment was accomplished with the vernier height gauge and an inside micrometer. Each nozzle block was then pinned to its slide rails using 3/8-in.-diameter dowel pins so that no rotational motion of slide rail with respect to nozzle block was possible. In spite of these precautions, some upward motion of the bottom nozzle block was detected in the early runs so that it was necessary to add an extra brace to this nozzle block.

The settling chamber is of 3/4-in. steel plate in order to stand the higher stagnation pressures which will be encountered in a later phase of the test program. There are two inlets into the settling chamber as shown in Fig. 2. One is a 4-in.-diameter opening in the upstream end, and the other is a 6-in.-diameter opening in one side. The 4-in.-diameter opening leads to a 3-in. air-operated control valve which is used for throttling the air in the settling chamber to the proper stagnation pressure. The 6-in. opening leads to a by-pass around the 3-in. valve. A 6-in. gate valve is in this by-pass so that the fairly high pressure drop across the 3-in. valve may be reduced for certain running conditions. The air which enters the settling chamber must pass through a 1-in.-square by 9-in.-long honeycomb which straightens out the flow prior to its entry into the secondary nozzle.

Both channels are sealed along the side walls with inflatable seals made of 1/8-in.-diameter rubber tubing. Due to structural difficulties, it is impossible to continue these inflatable seals to the very tip of the middle nozzle block so that from the tip to a point upstream 18 in. from the tip, this nozzle block is sealed by pressing felt between the nozzle block and the window. On the first few runs some leakage was present. However, by increasing the pressure on the inflatable seals and applying vacuum wax at several points, the leakage has been reduced to a point where it appears that no ill effects are present in the region of supersonic flow.

The instrumentation in the settling chamber consists of one static-pressure orifice located (Fig. 2) on the downstream end of the settling chamber. In addition, a Weston dial-type thermometer is located in the downstream end of the settling chamber.

Total-pressure profiles in the mixing region are obtained with a .041-in.-OD stainless-steel tube total head probe held in a probe holder which in turn is attached to the strut described in Reference 4. With this arrangement, it is possible to make fairly rapid traverses of the jet-mixing region. The vertical height of the probe is determined by viewing the probe through the window with a small telescope mounted on a height gauge.

## RESULTS AND DISCUSSION

For the experimental results which are presented here, the upper (4 in. x 4 in.) nozzle was set to give a Mach number of 2.5. The lower (2 in. x 4 in.) nozzle was set to give a Mach number of 2.0. The stagnation pressures in the upper and lower nozzles were, respectively, atmospheric and 12.5 in. Hg absolute so that the static pressures in the two jets were approximately equalized at 1.72 in. Hg absolute. The schlieren photograph in Fig. 4 (horizontal knife edge) shows the mixing region when the settling-chamber pressure for the lower nozzle was 12.6 in. Hg absolute. The dark band which represents the boundary layer on the upper surface of the middle nozzle block, and the light band which represents the boundary layer on the lower surface of the middle nozzle block, will be observed to leave the tip of the nozzle block and persist for a considerable distance downstream. Two discontinuities arise at the lip and one propagates into each stream. The white line which propagates into the upper channel represents a small compression wave. The wave which propagates into the lower channel consists first of a very faint light region followed by a sharper dark band. This light region represents a slight expansion of the gas followed by a small compression shock. A rather faint compression wave may be observed in the lower left-hand corner of this photograph. It will be noticed that the angle of inclination of this line, with respect to the flow direction, changes considerably as the wave passes from the lower to the upper jet.

Figure 5 is a schlieren photograph of the flow when the settling-chamber pressure is 17.01 in. Hg absolute. In this case a decided deflection of the mixing region in the direction of the upper jet is apparent. Figure 6, on the other hand, shows the flow with a settling-chamber pressure of 4.91 in. Hg absolute. In this case the mixing region turns sharply toward the lower channel.

Figure 7 is a plot of the ratio of the stagnation pressure behind a normal shock wave to the stagnation pressure of the main jet (atmospheric pressure) versus the vertical position of the probe as measured at several stations upstream and downstream from the lip.

The most striking feature of these traverses is the small rate of expansion of the mixing region. The thickness of the double boundary layer 0.42 in. upstream from the lip is about 0.73 in., while the thickness of the mixing region 10.72 in. downstream from the lip is about 0.87 in., giving an angle of spread of only about 0.7 degrees. The velocity ratio, which determines the rate of spread of an incompressible mixing region (Reference 5), was 0.9 for these measurements.

While the stagnation pressures and calculated Mach numbers indicated that the static pressures of the two streams were equalized, one must conclude from the schlieren picture of Fig. 5 and from the corresponding measurements of Fig. 7 that the static pressure in the lower jet was slightly higher than that in the upper. Static-pressure measurements have not yet been made for this configuration.

One also notes in the traverse 0.42 in. upstream from the lip that the pressure increases near the surface. Check points confirmed the two points nearest the surface in the upper traverse. Until further investigation, one can only remark that a pressure increase near the upper surface is consistent with a higher static pressure in the lower jet since some upstream propagation of the higher pressure would take place.

## THEORY OF COMPRESSIBLE TURBULENT MIXING

Many analyses of turbulent mixing, all of them phenomenological, have appeared since the first analysis by Tollmien[6] using Prandtl's mixing-length concept. All the theories involve assumptions and approximations, most of which cannot be segregated, so that a theory either agrees or does not agree with experiment; if it does not, the point of breakdown of the theory cannot in general be determined because of the number of simplifications which have been introduced.

Perhaps the simplest theories available are those proposed by Prandtl and Reichardt,[7,8] as a result of which the momentum equation takes the form of the heat-conduction equation. With similar simplifications and Prandtl number equal to unity, the energy equation also reduces to the heat-conduction equation with the stagnation temperature as the dependent variable. The theories contain two parameters, one of which must be evaluated from the observed rate of spread of the mixing region and the other establishing the origin of the coordinate system.

Surprisingly, the superposition of effects implied by the linearity of the differential equations appears to be borne out in practice, for those cases which have been investigated.[9] Chapman and Korst,[10] for instance, investigated the mixing of a compressible jet with still air and Weinstein[5] investigated the mixing of a low-speed jet in a moving stream. In both experiments, superposition appears to be realized.

The study for which this is an interim report will be a severe test of superposition because the boundary layers are thick, and there are gradients of both static and stagnation temperatures normal to the flow. In the above references, neither the boundary layer nor compressibility effects were large, so the results were not a very vigorous test of the superposition principle.

In a mixing region, it is standard practice to adopt Prandtl's boundary-layer approximations, to neglect all pressure gradients, and to assume that viscosity is constant. Therefore, the equation of motion takes the form

$$\frac{\partial u}{\partial t} + u\frac{\partial u}{\partial x} + v\frac{\partial u}{\partial y} = \nu\frac{\partial^2 u}{\partial y^2}, \qquad (1)$$

where u and v are instantaneous velocities, $\nu = \mu/\rho$ is the kinematic viscosity. Let $u = U + u'$, where U is the mean velocity with time and u' is the velocity fluctuation. Similarly, $v = V + v'$. Then Equation 1 becomes, after taking mean values,

$$U\frac{\partial U}{\partial x} + V\frac{\partial U}{\partial y} = \frac{1}{\rho}\frac{\partial}{\partial y}\left(\mu\frac{\partial U}{\partial y} - \rho\overline{u'v'}\right) - \frac{1}{\rho}\frac{\partial}{\partial x}\left(\rho\overline{u'^2}\right), \qquad (2)$$

where the bar signifies mean value with time. In this theory, variations and fluctuations in density are neglected.

Equation 2 has been simplified in two ways. In both ways, the terms

$$V\frac{\partial U}{\partial y}, \frac{\partial}{\partial x}\left(\rho\overline{u'^2}\right),$$

and the laminar friction term $\mu\partial U/\partial y$ are neglected. Then, Equation 2 becomes

$$U \frac{\partial U}{\partial x} = - \frac{1}{\rho} \frac{\partial}{\partial y} (\rho \overline{u'v'}) . \tag{3}$$

Now, $-\rho\overline{u'v'}$ is the Reynold's stress in the xy plane. Reichardt[8] approximates it by setting

$$\rho \overline{u'v'} = - \Lambda \frac{\partial (U^2)}{\partial y} \tag{3a}$$

and Equation 2 becomes

$$\frac{\partial (U^2)}{\partial x} = \frac{2\Lambda}{\rho} \frac{\partial^2 (U^2)}{\partial y^2} , \tag{4}$$

where $\Lambda$ is a mixing coefficient to be evaluated from experiment. This is the final form of the differential equation used in References 5 and 9 for incompressible jets.

Chapman and Korst, following Pai,[11] use a different linearization of Equation 2. They write, instead of Equation 3a,

$$\rho \overline{u'v'} = - \epsilon \frac{\partial U}{\partial y} \tag{5}$$

and, instead of $U\partial U/\partial x$, they write

$$\frac{U_1 + U_2}{2} \frac{\partial U}{\partial x} ,$$

i.e., they replace U by the average value of the two streams (Fig. 8), thus assuming that the variation of U is small. Then Equation 2 becomes

$$\frac{\partial U}{\partial x} = \frac{2\epsilon}{\rho (U_1 + U_2)} \frac{\partial^2 U}{\partial y^2} . \tag{6}$$

Equations 4 and 6 are of the same form, the coefficients on the right being assumed to be functions only of x, $U_2/U_1$, and (possibly) $M_2/M_1$. Whichever differential equation is used, the boundary conditions on U and $U^2$ will be similar. From here on we work with Equation 6, but the results are equally applicable to Equation 4 and at this point we cannot predict which will describe better the experimental results.

Korst, Page, and Childs[12] write the solution of Equation 6 for the

mixing of a compressible fluid with still air. In the following, we extend their results to the mixing of two streams as shown in Fig. 8.

The two streams have different (supersonic) Mach numbers ($M_1$ and $M_2$), static pressures ($p_{1o}$ and $p_{2o}$), velocities ($U_{1o}$ and $U_{2o}$), boundary-layer thicknesses ($\delta_{1o}$ and $\delta_{2o}$), and stagnation temperatures ($T_{o_1}$ and $T_{o_2}$). The two streams merge at the lip, and aft of any shocks and expansions the ambient pressures become $p_a$ and the directions of the two streams are again parallel, making an angle with their original directions determined by the ratio of their original ambient pressures. The initial conditions for the mixing are taken, as shown in Fig. 8, just downstream from the shocks and expansions at the lip.* We write

$$\zeta = \frac{y}{\delta_2}, \quad X = \frac{x}{\delta_2}, \quad \Phi = \frac{U}{U_2}, \quad \lambda = \frac{U_1}{U_2}.$$

Then Equation 6 becomes

$$\frac{\partial \Phi}{\partial X} = \frac{2\epsilon}{\rho U_2 \delta_2 (\lambda + 1)} \frac{\partial^2 \Phi}{\partial \zeta^2}. \tag{7}$$

Now, write

$$\epsilon = cX\delta_2 U_2 \frac{\lambda + 1}{2} \rho f(X). \tag{8}$$

In Reichardt's analysis[8] $\epsilon$ is taken proportional to x for the case of $\delta_1 = \delta_2 = 0$. Korst, Page and Childs[12] insert f (X) in Equation 8 and this analysis approaches Reichardt's at a great distance from the lip if we postulate that $f(X) \to 1$ as $X \to \infty$. Let

$$\xi = \xi(X) = c\int_0^X X\, f(X)\, dX, \tag{9}$$

where c is a constant to be determined. Then

$$\frac{\partial}{\partial X} = \frac{\partial}{\partial \xi} \cdot c\, X\, f(X)$$

*The initial conditions are taken just downstream from the lip because this theory for the mixing cannot possibly take into account the distortion of the boundary-layer velocity profiles caused by the flow around the lip resulting from static-pressure differences between the two streams or by the shocks and expansion originating at the lip. Figure 7, described in the previous section, shows, however, that this distortion is not great for small static-pressure differences.

and Equation 7 becomes

$$\frac{\partial \Phi}{\partial \xi} = \frac{\partial^2 \Phi}{\partial \zeta^2} \tag{10}$$

Equation 10 is the differential equation for heat condition with unit transfer coefficient. The solution of that equation for the proper boundary conditions becomes immediately applicable to the mixing problem.

In terms of the physical variables, the initial conditions are:

$$\begin{aligned} y &\leq -\delta_1, \; U = U_1 \\ y &\geq \delta_2, \; U = U_2 \\ 0 < y &< \delta_2, \; U = U_2 \Phi_2'(y) \\ -\delta_1 < y &< 0, \; U = U_1 \Phi_1'(y) \end{aligned}$$

and throughout $U = U_2 \, \Phi' \, (y)$.

Let $\delta_1/\delta_2 = \omega$ and $\Phi' \, (y) = \Phi \, (\zeta)$. Then, with $\xi = 0$ as the initial point, the initial and boundary conditions for the solution of Equation 10 are

$$\begin{aligned} \Phi(o,\zeta) &= \lambda \text{ for } -\infty < \zeta < -\omega \\ \Phi(0,\zeta) &= \Phi_1(\zeta) \text{ for } -\omega < \zeta < 0 \\ \Phi(0,\zeta) &= \Phi_2(\zeta) \text{ for } 0 < \zeta < 1 \\ \Phi(0,\zeta) &= 1 \text{ for } 1 < \zeta < \infty \\ \Phi(\xi, -\infty) &= \lambda \\ \Phi(\xi, +\infty) &= 1 \end{aligned} \Bigg\} \text{ for } \xi > 0 \tag{11}$$

Letting $\eta = \frac{\zeta}{2\sqrt{\xi}}$, $\eta_2 = \frac{1}{2\sqrt{\xi}}$, and $\eta_1 = \frac{-\omega}{2\sqrt{\xi}}$, we have

$$\eta - \eta_2 = \frac{\zeta - 1}{2\sqrt{\xi}} \text{ and } \eta - \eta_1 = \frac{\zeta + \omega}{2\sqrt{\xi}}.$$

The solution of Equation 10 satisfying conditions in Equations 11 is

$$\Phi(\Phi_1, \Phi_2, \eta_1, \eta_2, \eta) = \frac{1}{2}[1 + \operatorname{erf}(\eta - \eta_2)]$$

$$+ \frac{1}{\sqrt{\pi}} \int_{\eta-\eta_2}^{\eta} \Phi_2\left(\frac{\eta-\beta}{\eta_2}\right) e^{-\beta^2 d\beta} + \frac{\lambda}{2}[1 - \operatorname{erf}(\eta-\eta_1)] - \frac{1}{\sqrt{\pi}} \int_{\eta-\eta_1}^{\eta} \Phi_1\left(\frac{\eta-\beta}{\eta_1}\right) e^{-\beta^2 d\beta} \tag{12}$$

where

$$\text{erf}(z) = \frac{\sqrt{\pi}}{2} \int_0^z e^{-\beta^2} d\beta,$$

$\Phi_1(\zeta)$ and $\Phi_2(\zeta)$ are the measured initial distributions, and $\eta_1$ and $\eta_2$ are functions of x, c and f (X). The quantities c and f(X) must be determined from experiment.

Equation 12 is a solution of Equation 6 with boundary conditions in Equations 11. It is also a solution of Equation 4 with a redefinition of $\Phi_1$ and $\Phi_2$ in terms of $U^2$ instead of U. Only experiment can determine which (if either) describes the mixing process for two parallel supersonic flows with initial boundary layers.

In order to investigate temperature fluctuations, we may write in the energy equation for the form (p. 612 of Reference 13)

$$\frac{D}{Dt}\left(C_p T_1 + \frac{u^2}{2}\right) - \frac{1}{\rho}\frac{\partial p}{\partial t} = \frac{k}{\rho c_p}\frac{\partial^2}{\partial y^2}\left(C_p T_1 + \sigma \frac{u^2}{2}\right), \qquad (13)$$

where $T_1$ is the ambient temperature, $\sigma$ is the Prandtl number ($\sigma = C_p \mu/k$), and

$$\frac{D}{Dt} = \frac{\partial}{\partial t} + u\frac{\partial}{\partial x} + v\frac{\partial}{\partial y}.$$

As in Equation 1 we neglect pressure fluctuations and we set

$$u = U + u',\ v = V + v',\ T_1 = T + T',\ \text{and}\ \rho = \frac{p}{RT}. \qquad (14)$$

We substitute these relations in Equation 13 and take mean values. Then,

$$U\frac{\partial}{\partial x}\left(C_p T + \frac{U^2}{2} + \frac{\overline{u'^2}}{2}\right) + \overline{u'\frac{\partial}{\partial x}(C_p T' + Uu')}$$

$$V\frac{\partial}{\partial y}\left(C_p T + \frac{U^2}{2} + \frac{\overline{u'^2}}{2}\right) + \overline{v'\frac{\partial}{\partial y}(C_p T' + Uu')}$$

$$\frac{kR}{C_p p}\overline{(T + T')\frac{\partial^2}{\partial y^2}\left[C_p(T + T') + \sigma\frac{U^2}{2} + \sigma Uu' + \sigma\frac{u'^2}{2}\right]}$$

If we assume that the incompressible continuity equation is approximately valid, the expression

$$C_p\left[\frac{\partial u'}{\partial x} + \frac{\partial v'}{\partial y}\right]T' + \left[\frac{\partial u'}{\partial x} + \frac{\partial v'}{\partial y}\right]Uu' = 0$$

is added to the left side and T' is neglected in the numerator in the right, then the equation becomes

$$\left[U\frac{\partial}{\partial x} + V\frac{\partial}{\partial y}\right]\left[C_pT + \frac{U^2}{2} + \frac{\overline{u'^2}}{2}\right] + C_p\frac{\partial}{\partial x}\overline{u'T'} + C_p\frac{\partial}{\partial y}\overline{v'T'}$$

$$+ \frac{\partial}{\partial x}(\overline{Uu'^2}) + \frac{\partial}{\partial y}(\overline{Uu'v'}) = \frac{k}{\rho C_p}\frac{\partial^2}{\partial y^2}\left[C_pT + \sigma\frac{U^2}{2} + \sigma\frac{\overline{u'^2}}{2}\right]. \quad (15)$$

In this equation we neglect $\overline{u'^2}$ compared with $U^2$,

$$C_p\frac{\partial}{\partial x}\overline{u'T'} \text{ and } C_p\frac{\partial}{\partial x}(\overline{Uu'^2})$$

compared with the other two turbulent transfer terms, and $V\frac{\partial}{\partial y}(\ )$ compared with $U\frac{\partial}{\partial x}(\ )$. Further, we set

$$\left.\begin{aligned}\overline{v'T'} &= -\frac{k_t}{\rho C_p}\frac{\partial T}{\partial y}\\ \overline{u'v'} &= -\frac{\epsilon}{\rho}\frac{\partial U}{\partial y}\end{aligned}\right\}. \quad (16)$$

Then Equation 15 becomes

$$U\frac{\partial}{\partial x}\left(C_pT + \frac{U^2}{2}\right) = \frac{k}{\rho C_p}\frac{\partial^2}{\partial y^2}\left(C_pT + \sigma\frac{U^2}{2}\right) + \frac{k_t}{\rho C_p}\frac{\partial^2}{\partial y^2}\left(C_pT + \frac{C_p\epsilon}{k_t}U^2\right).$$

If we write the turbulent Prandtl number $\sigma_t = C_p\epsilon/k_t$ and neglect laminar transfer compared with turbulent, we get

$$U\frac{\partial}{\partial x}\left(C_pT + \frac{U^2}{2}\right) = \frac{k_t}{\rho C_p}\frac{\partial^2}{\partial y^2}\left(C_pT + \sigma_t\frac{U^2}{2}\right). \quad (17)$$

Now let $\sigma_t = 1$, $U = (U_1 + U_2)/2$ and write $C_pT_o = C_pT + \frac{U^2}{2}$, where $T_o$ is the stagnation temperature. Then

$$\frac{\partial T_o}{\partial x} \qquad \frac{2k_t}{\rho C_p U_2(\lambda + 1)} \frac{\partial^2 T_o}{\partial y^2} . \tag{18}$$

This equation is identical in form with Equation 6. Further, the boundary conditions on $T_o$ are given by Equation 11 with only a change in the symbols. Hence, within the framework of the above simplifications, Equation 12 describes the spreading of the stagnation temperature as well as of the momentum. The difference in the rates of spread of heat and momentum caused by the deviation of the turbulent Prandtl number from unity will be taken into account by a change in the factors to be evaluated by experiment.

The above theories will be applied to the results presented in the previous section and to other test results to be obtained for velocity and for temperature distributions in the mixing regions.

## FUTURE PROGRAM

The future program consists of the following items:

1. Total head and stagnation-temperature profiles and optical surveys in the mixing regions and in the vicinity of the lip for a representative series of Mach number and static-pressure ratios through the entire range possible with the apparatus.

2. Pressurization of the air supplies of both jets up to at least 45 psi absolute.

3. Introduction of boundary-layer control on one or both center-block surfaces to simulate higher Reynolds numbers.

4. Investigation of the feasibility of velocity-fluctuation measurements in the mixing region.

REFERENCES


1. Forstall, W., Jr., and A. H. Shapiro, "Momentum and Mass Transfer in Coaxial Gas Jets," J. Appl. Mech., 10:399-408 (1950).
2. Krzywoblocki, M. Z., "Jets," U.S. Naval Ordnance Test Station TM No. 1576 (1953).
3. Amick, J. L., H. P. Liepman, and T. H. Reynolds, "Development of a Variable Mach Number Sliding Block Nozzle and Evaluation in the Mach Number Range 1.3 to 4.0," WADC Tech. Rept. No. 55-88 (March 1955).
4. Liepman, H. P., J. S. Murphy, and J. H. Nourse, "A Physical Description of a Variable Mach Number 4 x 4 Inch Pilot Corner Nozzle," Univ. of Mich. WTM 246 (December 1953).
5. Weinstein, Alvin S., "Diffusion of Momentum from Free and Confined Slot Jets into Moving Secondary Streams," Carnegie Inst. of Tech., Scientific Rept. No. 2, Contract AF 18(600)-969.
6. Tollmien, W., "Turbulent Mixing," NACA TM 1085 (1945), originally published in Z.A.M.M. (1926).
7. Prandtl, L., "Bemerkungen zur Theorie der freien Turbulenz," Z.A.M.M., 22:241-3 (1942).
8. Reichardt, H., "Gesetzmässigkeit der freien Turbulenz," V.D.I. Forschungsheft 414 Serie B, Vol. 13 (1942).
9. Baron, L. and L. G. Alexander, "Mixing of Coaxial Jets," Chem. Eng. Prog. 47:181-4 (1951).
10. Chapman, A. J. and H. H. Korst, "Free Jet Boundary with Consideration of Initial Boundary Layer," Proc. 2nd Nat. Cong. for Appl. Mech., Univ. of Mich. (1955).
11. Pai, S. I., "Two Dimensional Jet Mixing of a Compressible Fluid," J. Aero. Sci., 16:463-9 (1949).
12. Korst, H. H., R. H. Page, and M. E. Childs, "Compressible Two-Dimensional Jet Mixing at Constant Pressure," M. E. Tech. Note 392-1, Contract AF 18(600)-392, Univ. of Ill. (1954).
13. Goldstein, S., Ed., Modern Developments in Fluid Dynamics, (Oxford Engineering Science Series), 2 vols., 1938.

# 4"x 4" CORNER NOZZLE MODIFICATION FOR JET MIXING

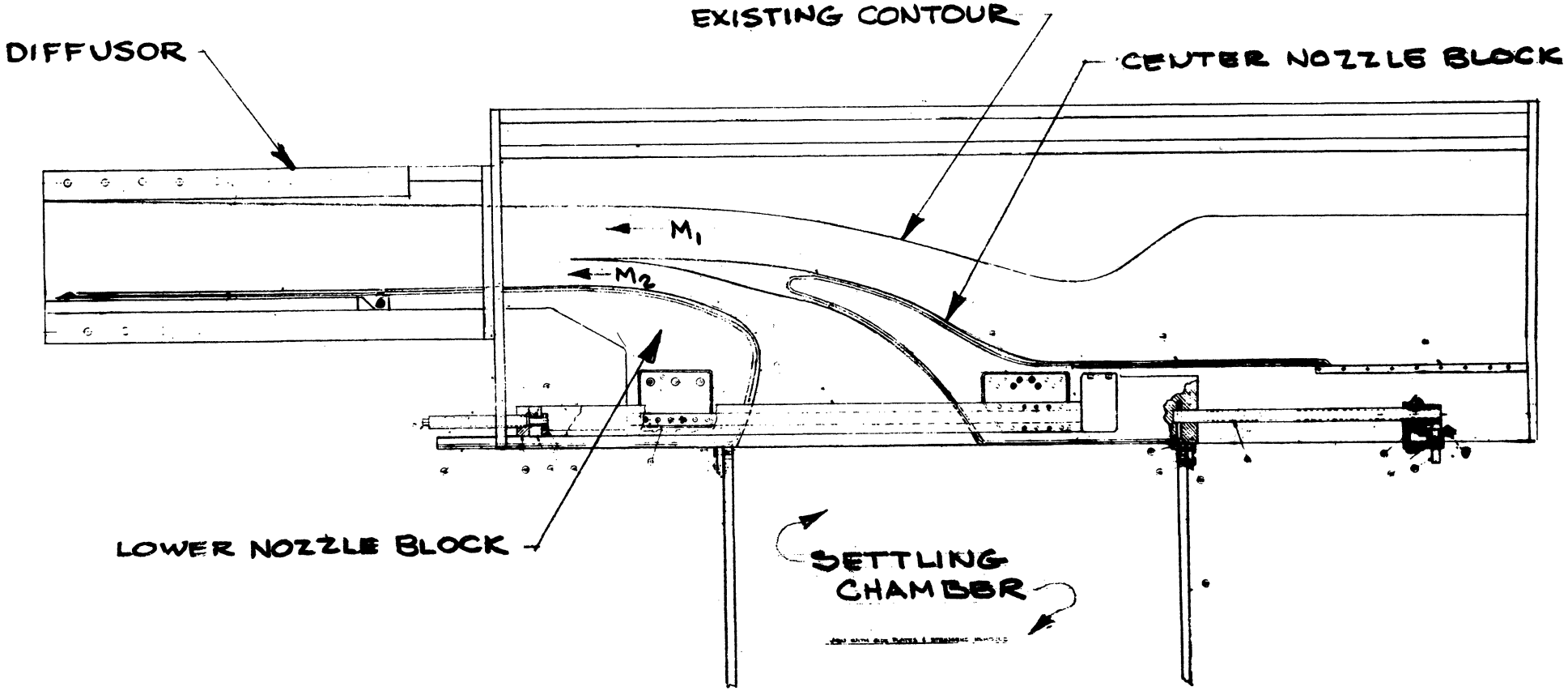


Fig. 1.

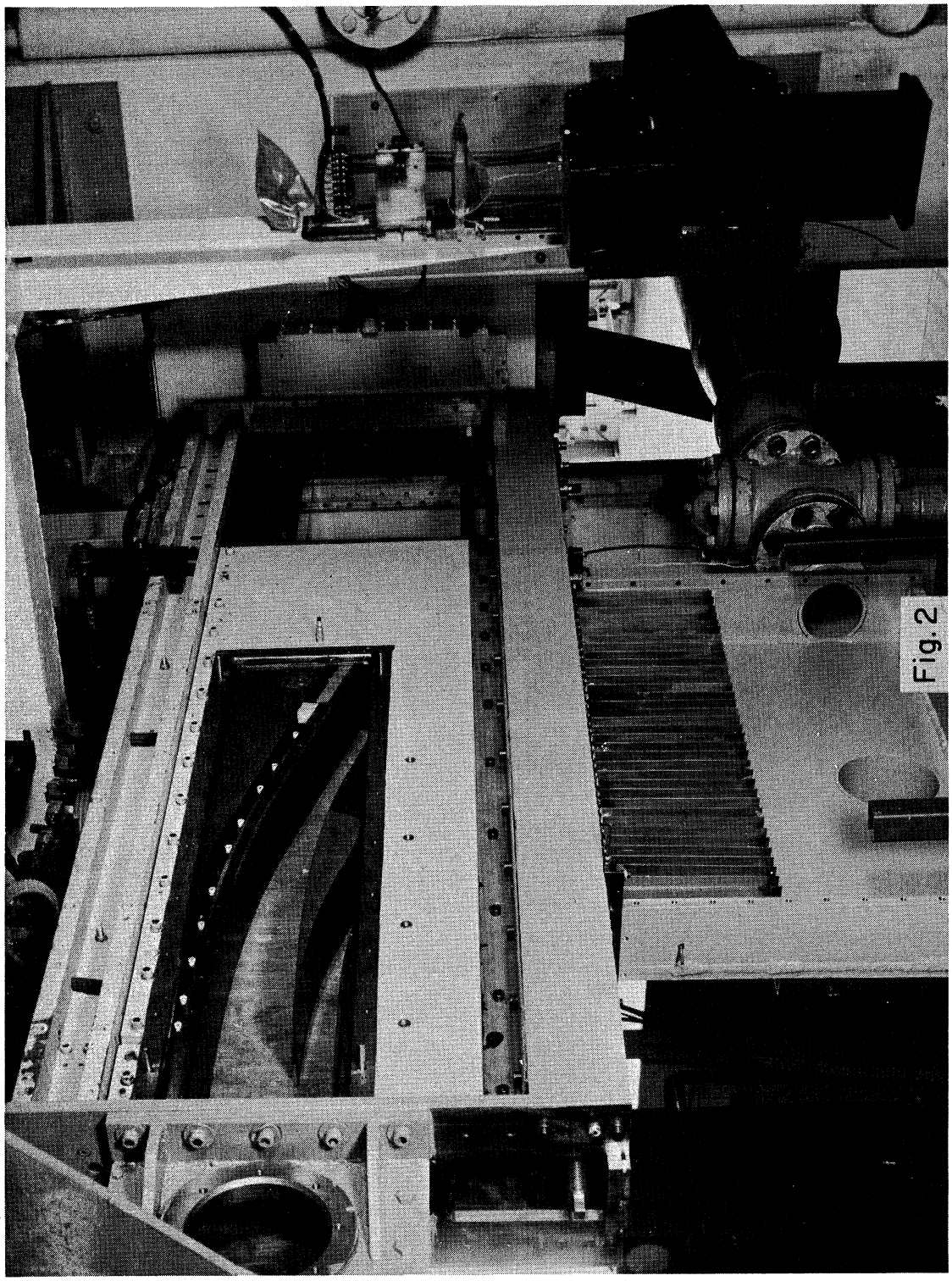

Fig. 2

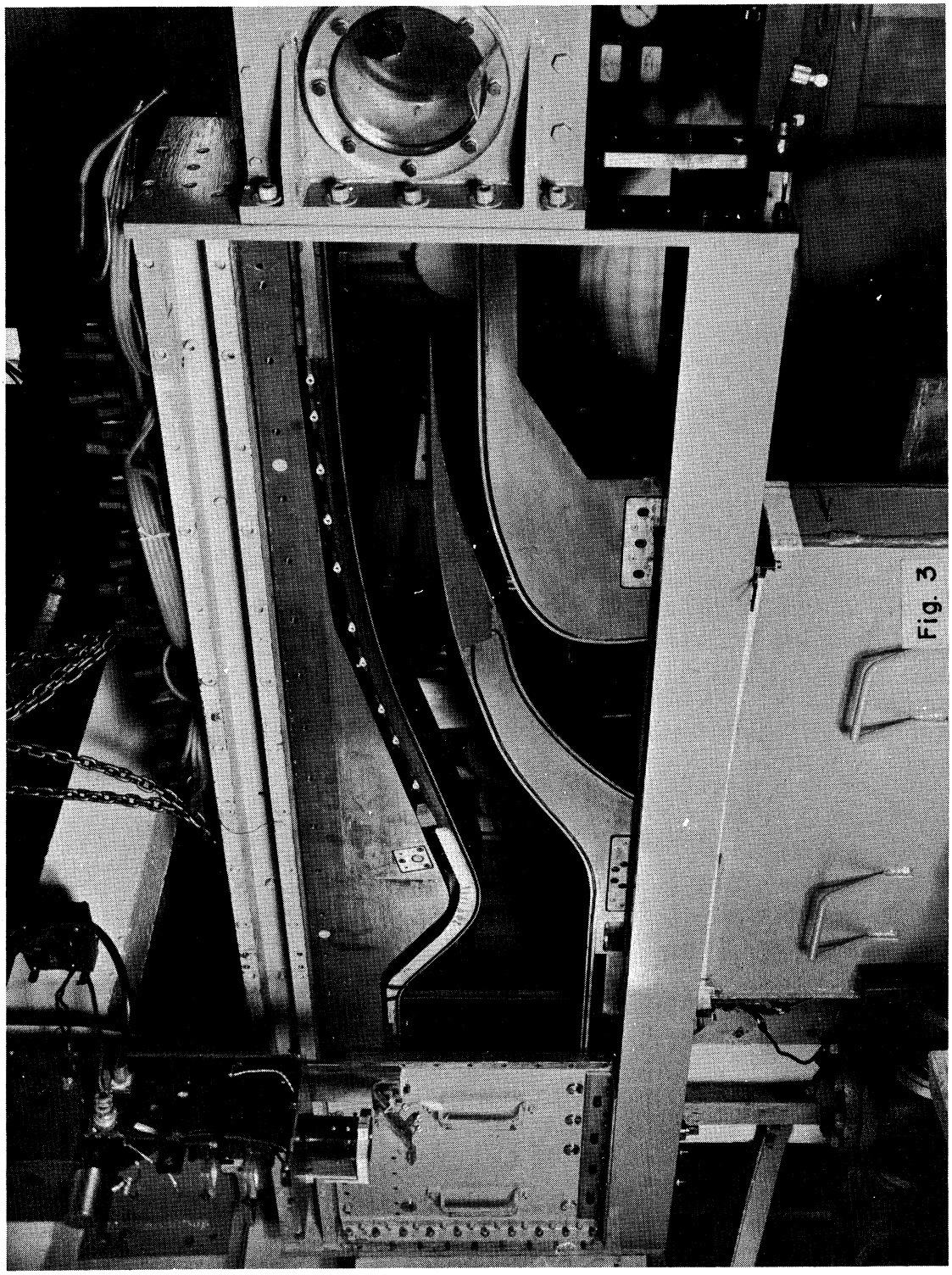

Fig. 3

Fig. 4

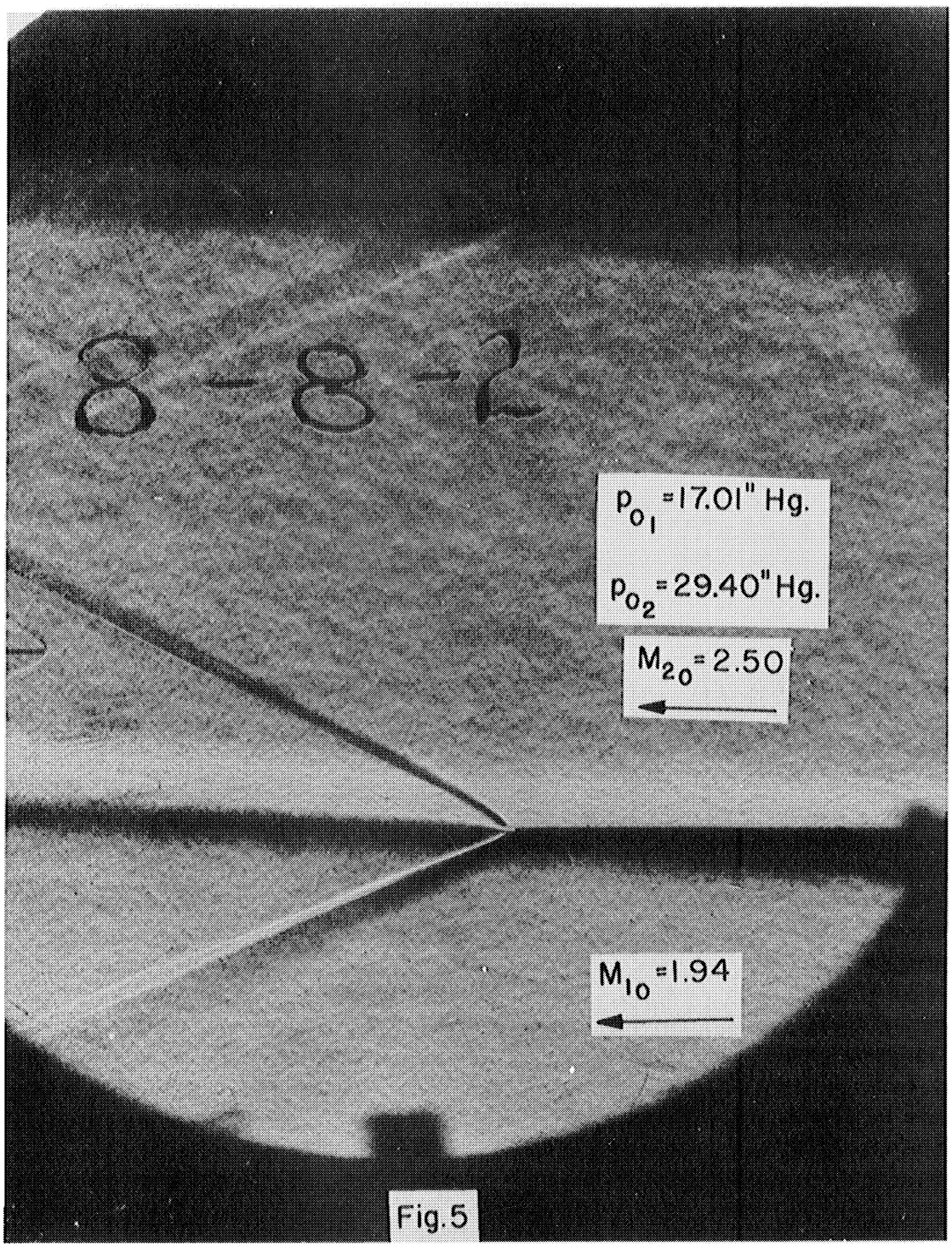


Fig. 5

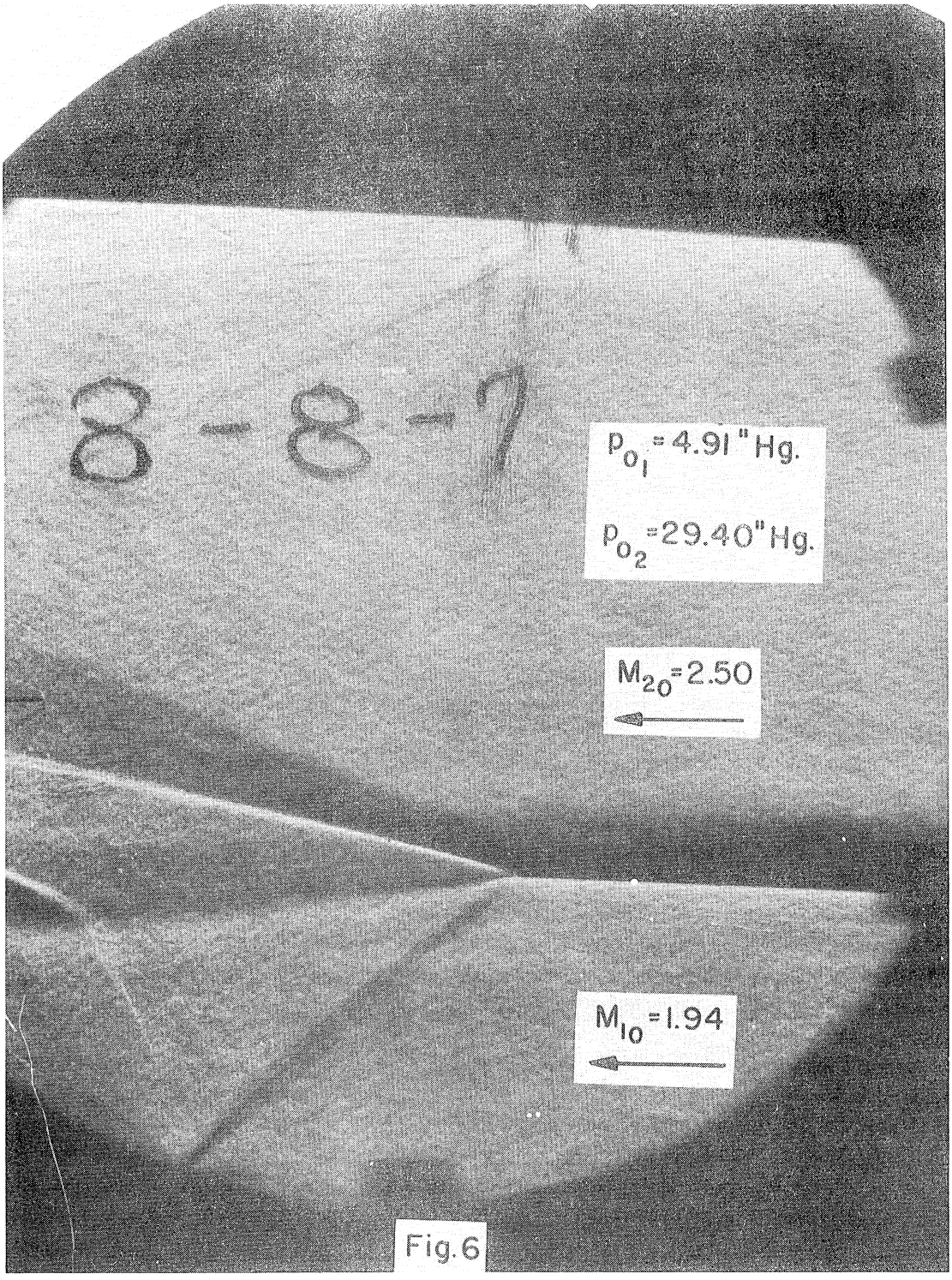


Fig. 6

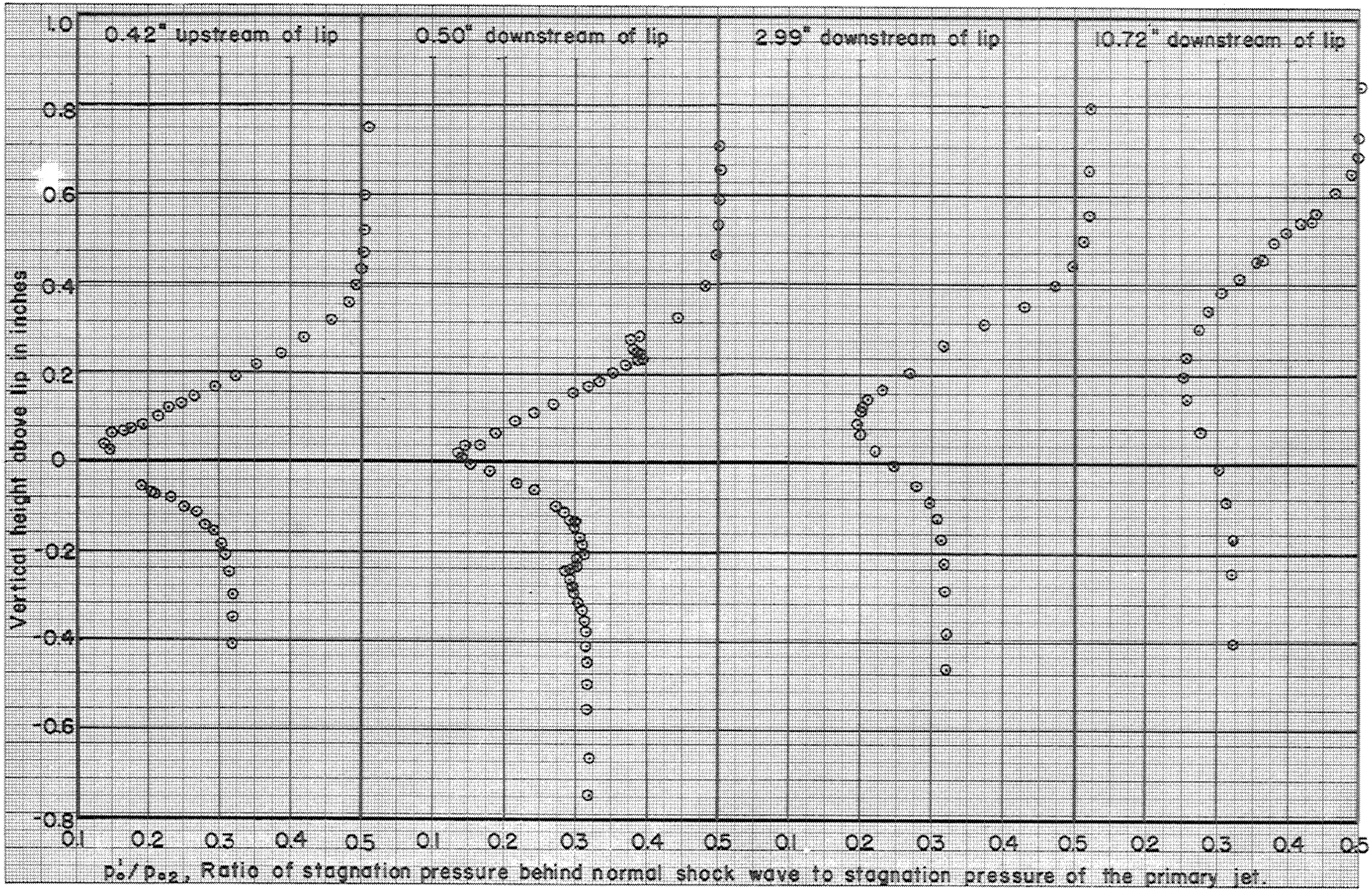
0.42" upstream of lip
0.50" downstream of lip
2.99" downstream of lip
10.72" downstream of lip
Vertical height above lip in inches
1.0
0.8
0.6
0.4
0.2
0
-0.2
-0.4
-0.6
-0.8
0.1 0.2 0.3 0.4 0.5 0.1 0.2 0.3 0.4 0.5 0.1 0.2 0.3 0.4 0.5 0.2 0.3 0.4 0.5
$p_o'/p_{o2}$, Ratio of stagnation pressure behind normal shock wave to stagnation pressure of the primary jet.

Fig. 7

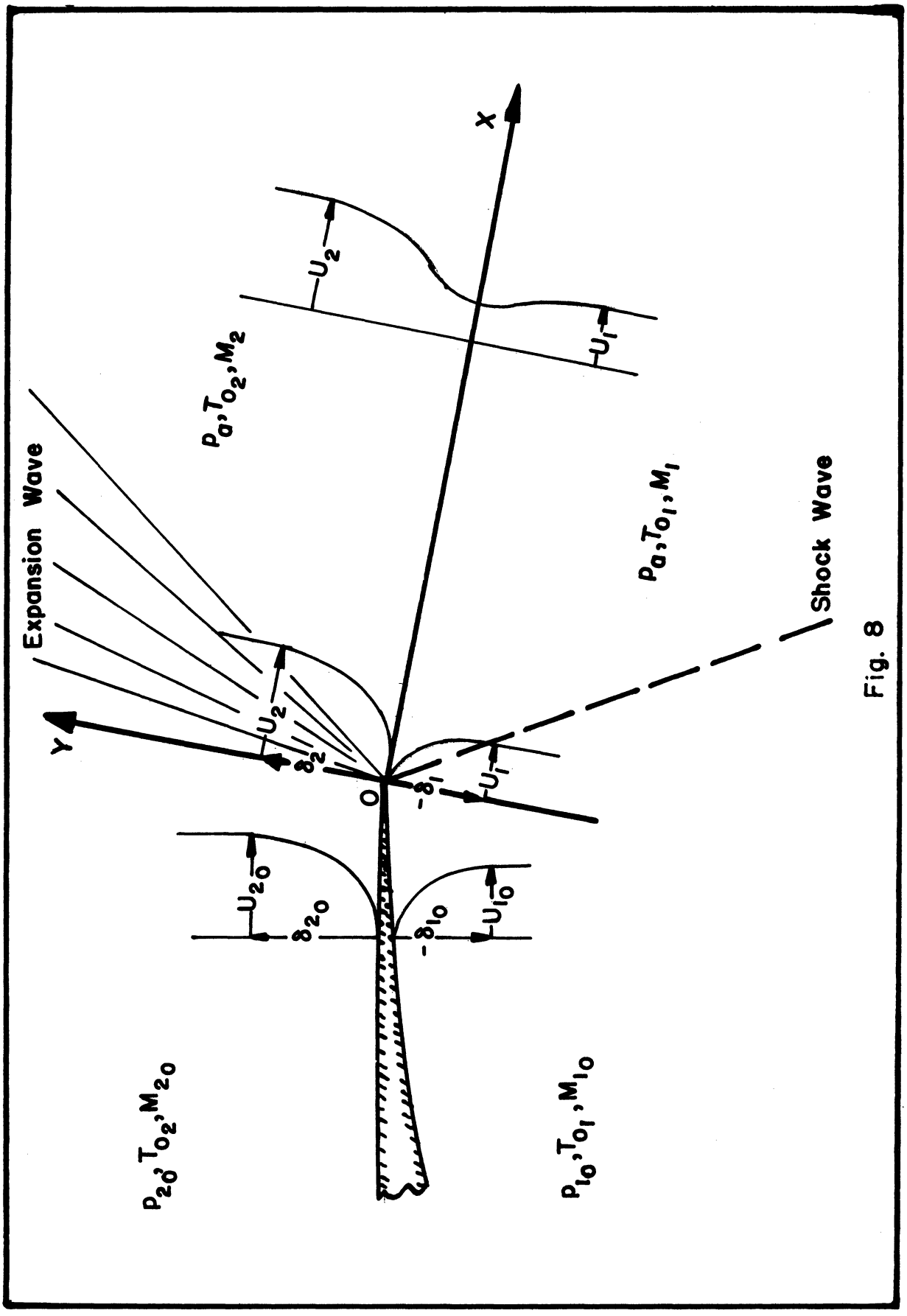
Expansion Wave
Shock Wave
X
Y
O
$U_2$
$U_1$
$\delta_2$
$-\delta_1$
$U_{20}$
$U_{10}$
$\delta_{20}$
$-\delta_{10}$
$p_a, T_{o_2}, M_2$
$p_a, T_{o_1}, M_1$
$p_{20}, T_{o_2}, M_{20}$
$p_{10}, T_{o_1}, M_{10}$

Fig. 8